PNAS RESEARCH ARTICLE | CELL BIOLOGY

Accumulation of annexin A2 and S100A10 prevents apoptosis of apically delaminated, transformed epithelial cells

Shoko Ito[a,b], Keisuke Kuromiya[a], Miho Sekai[a,b], Hiroaki Sako[a], Kazuhito Sai[a], Riho Morikawa[a,b], Yohei Mukai[c], Yoko Ida[c], Moe Anzai[c], Susumu Ishikawa[d], Kei Kozawa[a], Takanobu Shirai[a,d], Nobuyuki Tanimura[a], Kenta Sugie[a,b], Junichi Ikenouchi[e], Motoyuki Ogawa[f], Isao Naguro[f], Hidenori Ichijo[f], and Yasuyuki Fujita[a,1]

Edited by Denise Montell, University of California, Santa Barbara, CA; received May 6, 2023; accepted September 12, 2023

In various epithelial tissues, the epithelial monolayer acts as a barrier. To fulfill its function, the structural integrity of the epithelium is tightly controlled. When normal epithelial cells detach from the basal substratum and delaminate into the apical lumen, the apically extruded cells undergo apoptosis, which is termed anoikis. In contrast, transformed cells often become resistant to anoikis and able to survive and grow in the apical luminal space, leading to the formation of multilayered structures, which can be observed at the early stage of carcinogenesis. However, the underlying molecular mechanisms still remain elusive. In this study, we first demonstrate that S100A10 and ANXA2 (Annexin A2) accumulate in apically extruded, transformed cells in both various cell culture systems and murine epithelial tissues in vivo. ANXA2 acts upstream of S100A10 accumulation. Knockdown of ANXA2 promotes apoptosis of apically extruded RasV12-transformed cells and suppresses the formation of multilayered epithelia. In addition, the intracellular reactive oxygen species (ROS) are elevated in apically extruded RasV12 cells. Treatment with ROS scavenger Trolox reduces the occurrence of apoptosis of apically extruded ANXA2-knockdown RasV12 cells and restores the formation of multilayered epithelia. Furthermore, ROS-mediated p38MAPK activation is observed in apically delaminated RasV12 cells, and ANXA2 knockdown further enhances the p38MAPK activity. Moreover, the p38MAPK inhibitor promotes the formation of multilayered epithelia of ANXA2-knockdown RasV12 cells. These results indicate that accumulated ANXA2 diminishes the ROS-mediated p38MAPK activation in apically extruded transformed cells, thereby blocking the induction of apoptosis. Hence, ANXA2 can be a potential therapeutic target to prevent multilayered, precancerous lesions.

annexin A2 | S100A10 | apical extrusion | RasV12-transformed | apoptosis

Significance

When epithelial cells detach from the basal substratum and are extruded into the apical lumen, they will be subjected to physical stresses including the increased reactive oxygen species (ROS) and eventually undergo apoptosis. Oncogenically transformed epithelial cells often become resistant to apoptosis upon apical extrusion; however, the underlying molecular mechanisms still remain obscure. Here, we demonstrate that ANXA2 (Annexin A2) accumulates in apically extruded transformed cells. In addition, ANXA2 contributes to resistance to ROS-mediated apoptosis by suppressing p38MAPK, a stress-activated protein kinase, thereby promoting the formation of multilayered epithelia. Thus, ANXA2 is a potential therapeutic target to prevent the development of precancerous lesions.

In a variety of epithelial tissues such as gut, lung, pancreas, and mammary gland, the epithelial monolayer plays a crucial role as a barrier to block the pathogens or harmful substances from invading the inside of the body (1, 2). The formation of apicobasal polarity is one of the characteristics of the monolayered epithelial cells; the apical side of epithelial cells faces the lumen of the epithelium, whereas the basal side adheres to the basement membrane and underlying matrix (3). The apical cell extrusion is one of the important homeostatic mechanisms for the maintenance of epithelial integrity. For example, at high cell density, cells are often apically extruded to alleviate the overcrowding condition (4, 5). In addition, when oncogenic transformation occurs within the epithelium, the newly emerging transformed cells are extruded from the apical side of the epithelial monolayer through cell competition with the surrounding normal cells (6, 7). Upon apical extrusion, cells will lose the attachment with the basement membrane and basal matrix proteins, leading to a loss of survival signaling through integrin-based adhesions (8, 9). Apically extruded cells will be also subjected to physical stresses including the increased reactive oxygen species (ROS) (10). Accordingly, apically extruded normal epithelial cells undergo apoptosis, which is termed anoikis (11–14). In contrast, transformed cells often become resistant to anoikis (13, 15, 16) and able to survive and grow in the apical luminal space, leading to the formation of multilayered structures (17–20). However, it is not clearly understood which molecules or signaling pathways are modulated in apically transformed cells to prevent the induction of apoptosis.

Annexin A2 (ANXA2) is a member of the annexin family, a group of calcium-dependent membrane-bound molecules composed of a variable N-terminal domain and conserved C-terminal annexin core domains (21, 22). ANXA2 interacts with S100A10, a member of the S100 protein family characterized by the EF-hand motifs and helix-loop-helix motifs (23, 24). Two ANXA2 molecules and a homodimer of S100A10 form a heterotetrameric complex, and the absence of ANXA2 posttranscriptionally destabilizes S100A10 (25). The AXAN2/S100A10 complex localizes to the plasma membrane by binding the core domains of ANXA2

Author contributions: S. Ito and Y.F. designed research; S. Ito, K. Kuromiya, M.S., H.S., K. Sai, R.M., Y.M., Y.I., M.A., S. Ishikawa, K. Kozawa, T.S., N.T., K. Sugie, J.I., M.O., I.N., and H.I. performed research; S. Ito, K. Kuromiya, and Y.F. analyzed data; and S. Ito and Y.F. wrote the paper.

The authors declare no competing interest.

This article is a PNAS Direct Submission.

Copyright © 2023 the Author(s). Published by PNAS. This article is distributed under Creative Commons Attribution-NonCommercial-NoDerivatives License 4.0 (CC BY-NC-ND).

[1]To whom correspondence may be addressed. Email: fujita@monc.med.kyoto-u.ac.jp.

This article contains supporting information online at https://www.pnas.org/lookup/suppl/doi:10.1073/pnas.2307118120/-/DCSupplemental.

Published October 16, 2023.

with membrane phospholipids (24). ANXA2/S100A10 are involved in multiple cellular processes, including membrane trafficking, cytoskeletal organization, proliferation, and cell death (21, 26, 27). Expression of ANXA2 and S100A10 is elevated in various types of cancer (28, 29). Several studies have reported that the upregulated expression of ANXA2 or S100A10 induces antiapoptotic properties, which can lead to resistance against cancer treatment (30–34). However, the role of ANXA2/S100A10 at the early stage of carcinogenesis remains largely unknown.

In this study, we demonstrate that ANXA2 and S100A10 accumulate in apically extruded, transformed cells. The accumulated ANXA2/S100A10 suppress the ROS-mediated apoptosis, thereby promoting the multilayered, transformed epithelial structures, which is often observed at the earlier stage of cancer development.

Results

S100A10 Accumulates in Transformed Cells That Are Apically Extruded from the Epithelial Monolayer. To identify proteins that are involved in the apical extrusion of transformed cells, we performed phage antibody display screening using normal and RasV12-transformed Madin–Darby canine kidney (MDCK) epithelial cells (Fig. 1*A*). After a series of screenings, we isolated one antibody (1D2) that recognized some of RasV12 cells under the coculture condition with normal cells (white arrowheads) (Fig. 1*B*). Confocal microscopic analyses revealed that the 1D2 antibody specifically recognized apically extruded RasV12 cells that had detached from the basal substratum, but not RasV12 cells remaining within the epithelial monolayer (Fig. 1 *C* and *D*). 1D2 antibody immunoprecipitated a protein of 11 kDa that was detected by western blotting with 1D2 (Fig. 1 *E* and *F*; white and black arrowheads), and mass spectrometric analysis revealed that the 11-kDa protein was S100A10. We then established MDCK-RasV12 cells stably expressing S100A10-shRNA. Knockdown of S100A10 strongly diminished the 11-kDa band in western blotting which was detected by 1D2 antibody or commercially obtained anti-S100A10 antibody (Fig. 1*G*), validating that 1D2 indeed recognizes S100A10. Similarly, 1D2 immunofluorescence in apically extruded RasV12 cells was profoundly reduced by S100A10-knockdown (Fig. 1*H*). During apical extrusion, RasV12 cells first change their morphology; the height of RasV12 cells along the apicobasal axis becomes higher than that of the surrounding normal cells, with their nucleus apically shifted (Fig. 1*C* and *SI Appendix*, Fig. S1*A*) (6). The accumulation of S100A10 was observed in RasV12 cells that completely detached from the basal substratum and translocated into the apical lumen but not in RasV12 cells that showed morphological changes but still attached to the basal matrix (*SI Appendix*, Fig. S1*A*). This result suggests that the detachment from the basal substratum is required for the accumulation of S100A10. Apical delamination of transformed cells also occurs, though less frequently, when transformed cells are cultured alone for a long duration (18). Accumulation of S100A10 was observed in apically extruded RasV12 cells under the single culture condition of RasV12-transformed MDCK or human pancreatic ductal epithelial (HPDE) cells (Fig. 1 *I* and *J* and *SI Appendix*, Fig. S1 *B–D*). When cells were cultured in a nonconfluent condition where extrusion did not occur, the expression level of S100A10 was comparable between normal and RasV12 cells (*SI Appendix*, Fig. S1*E*). Accumulation of S100A10 was also observed in apically extruded Src-transformed cells (*SI Appendix*, Fig. S1 *F* and *G*). In addition, the comparable S100A10 accumulation was detected in apically delaminated human pancreatic adenocarcinoma PANC-1 and AsPC-1 cells that were cultured alone (Fig. 1 *K* and *L* and *SI Appendix*, Fig. S1 *H* and *I*). Immunofluorescence of β-catenin, E-cadherin, or gp135, other membrane-anchored or transmembrane proteins, was not elevated in apically extruded RasV12 cells (*SI Appendix*, Fig. S1*J*). Furthermore, in CK19-RasV12 cell competition model mice (35), S100A10 was accumulated in RasV12-expressing cells that were apically extruded from the pancreatic ductal and lung bronchial epithelia (Fig. 1*M* and *SI Appendix*, Fig. S1*K*). Collectively, these data indicate that the accumulation of S100A10 in apically delaminated transformed cells is a prevalent process that was observed both in vitro and in vivo.

ANXA2 Also Accumulates in Apically Extruded Transformed Cells and Acts Upstream of S100A10. We next analyzed the localization and expression of ANXA2, which binds and cofunctions with S100A10, in apically extruded transformed cells. Immunofluorescence analysis showed that similarly to S100A10, the fluorescence intensity of ANXA2 was significantly elevated in apically extruded RasV12-transformed cells from the monolayer of normal MDCK epithelial cells, which was diminished by ANXA2-knockdown (Figs. 2 *A* and *B* and 3*A*). The accumulation of ANXA2 was also observed in apically delaminated RasV12 cells under the single culture condition (Fig. 2 *C* and *D*). When cells were cultured in a nonconfluent condition, the expression level of ANXA2 was comparable between normal and RasV12 cells (*SI Appendix*, Fig. S2*A*). ANXA2 colocalized with S100A10 mainly at the plasma membrane of the apically extruded cells (Fig. 2*E*). Accumulation of ANXA2 was also observed in apically delaminated RasV12-transformed HPDE cells, PANC-1 cells, or AsPC-1 cells (Figs. 2 *F* and *G* and 3*C* and *SI Appendix*, Fig. S2 *B* and *C*). Moreover, ANXA2 was accumulated in apically extruded RasV12-expressing cells in the pancreatic and bronchial epithelium of CK19-RasV12 mice (Fig. 2*H* and *SI Appendix*, Fig. S2*D*). Thus, both S100A10 and ANXA2 accumulated in apically extruded transformed cells under the various experimental conditions.

Furthermore, we showed by western blotting that the protein expression levels of S100A10 and ANAX2 increased as RasV12-transformed cells started forming multilayered structures after longer incubations (*SI Appendix*, Fig. S3 *A* and *B*). Using RT-qPCR, we found that the mRNA of both S100A10 and ANAX2 increased in RasV12 cells when they formed bilayered epithelia (*SI Appendix*, Fig. S3 *C* and *D*). The analyses with RNAscope also confirmed that the expression of S100A10 and ANXA2 was elevated in apically extruded PANC-1 cells at the mRNA level (*SI Appendix*, Fig. S3 *E* and *F*). Similarly, ANXA2 mRNA increased in apically extruded RasV12 cells in the lung bronchial epithelium (*SI Appendix*, Fig. S3*G*). Thus, the expression of S100A10 and ANXA2 is up-regulated at both mRNA and protein levels in apically extruded transformed cells. Next, we cultured RasV12 cells under the nonadherent condition and found that the mRNA level of S100A10 and ANXA2 was not significantly different between adherent and nonadherent RasV12 cells (*SI Appendix*, Fig. S3 *H* and *I*), suggesting that the detachment from the basal substratum is not sufficient to trigger the upregulation of S100A10 and ANXA2 and that the attachment to the underlying epithelial cells may also be required.

Under the crowded condition, normal cells can also be apically extruded, a process termed crowding-induced extrusion (4, 5). When normal MDCK cells are cultured alone at high cell density, apical extrusion occasionally occurs, and apically extruded normal cells eventually die (4). We then cultured normal cells at high density in the presence of cell death inhibitors and found that either S100A10 or ANXA2 accumulated in apically extruded normal cells

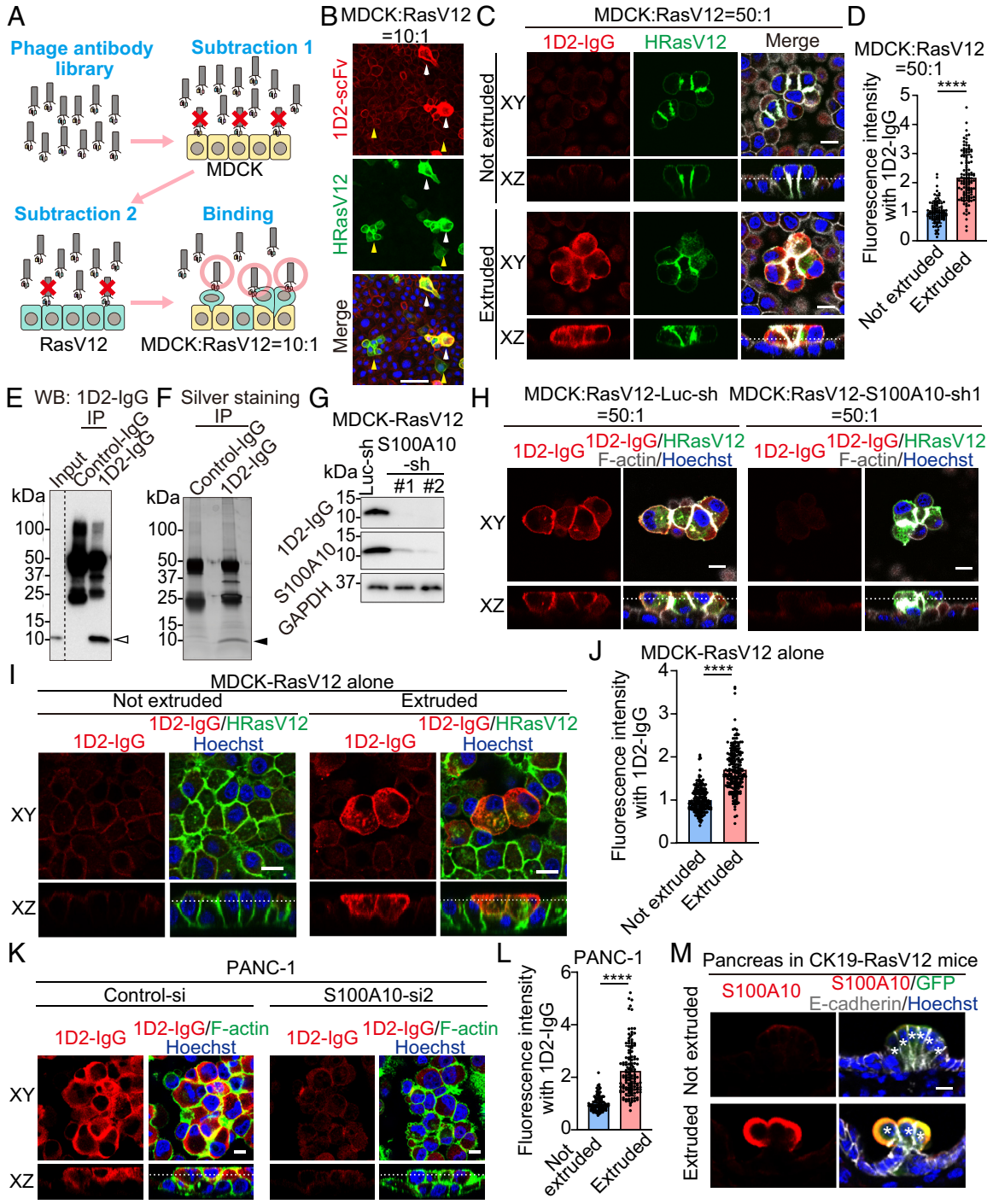

Fig. 1. S100A10 is accumulated in apically extruded, transformed cells. (*A*) Schematics for phage antibody display screening to identify antibodies that bound to molecules of which expression or membrane localization is up-regulated under the coculture condition of normal and RasV12-transformed MDCK cells. (*B* and *C*) Immunofluorescence images of RasV12 cells with 1D2-single chain Fv (scFv) (*B*) or 1D2-IgG (*C*). The phage antibody isolated by the screening is 1D2-scFv. 1D2-IgG was generated by adding the constant regions of IgG to 1D2-scFv, which was used in the following immunofluorescence analyses. MDCK-pTR GFP-RasV12 cells were cocultured with normal MDCK cells at the indicated ratio. After 24 h of doxycycline treatment, cells were stained with1D2-scFv (red) (*B*) or 1D2-IgG (red) (*C*), Hoechst (blue), and/or Alexa Fluor 647-conjugated phalloidin (gray). (*B*) White and yellow arrowheads indicate RasV12 cells with and without intense 1D2-scFv immunofluorescence, respectively. (*D*) Quantification of the 1D2-IgG fluorescence intensity in (*C*). Values are expressed as a ratio relative to Not extruded. Data are mean ± SD. ****$P < 0.0001$ (Mann–Whitney test); n = 98 and 124 cells from three independent experiments. (*E* and *F*) Identification of S100A10 by immunoprecipitation. Lysates from normal MDCK cells were subjected to immunoprecipitation with 1D2-IgG, followed by western blotting with 1D2-IgG (*E*) or silver staining (*F*). The black arrowhead indicates the band analyzed by mass spectrometry. (*G* and *H*) Validation of S100A10 as an epitope protein of 1D2 antibody. (*G*) Lysates from MDCK-pTR GFP-RasV12 Luc-shRNA, S100A10-shRNA1, or S100A10-shRNA2 cells were analyzed by western blotting with 1D2-IgG, commercially obtained anti-S100A10 antibody, or anti-GAPDH antibody. (*H*) MDCK-pTR GFP-RasV12 Luc-shRNA or S100A10-shRNA1 cells were cocultured with normal cells, and cells were stained with 1D2-IgG (red), Alexa Fluor 647-conjugated phalloidin (gray), and Hoechst (blue). (*I–L*) Immunofluorescence analyses of S100A10. (*I* and *K*) Immunofluorescence images of S100A10 in apically delaminated RasV12 cells (*I*) and PANC-1 cells (*K*) under the single culture condition. MDCK-pTR GFP-RasV12 (*I*) or PANC-1 (*K*) cells were cultured alone and stained with 1D2-IgG (red), Hoechst (blue), and/or Alexa Fluor 488-conjugated phalloidin (green). (*J* and *L*) Quantification of the fluorescence intensity of S100A10 in (*I*) and (*K*). Values are expressed as a ratio relative to Not extruded. Data are mean ± SD. ****$P < 0.0001$ (Mann-Whitney test); (*J*) n = 201 and 206 cells and (*L*) n = 103 and 131 cells from three independent experiments. (*M*) Immunofluorescence images of S100A10 in apically extruded RasV12-expressing cells in the murine pancreatic epithelium. At 7 d after the induction of RasV12 expression by tamoxifen administration, the pancreatic tissue samples from CK19-RasV12-GFP mice were stained with anti-S100A10 (red), anti-GFP (green), and anti-E-cadherin (gray) antibodies, and Hoechst (blue). The asterisks indicate RasV12-expressing cells. [Scale bars, 50 μm (*B*) and 10 μm (*C*, *H*, *I*, *K*, and *M*).]

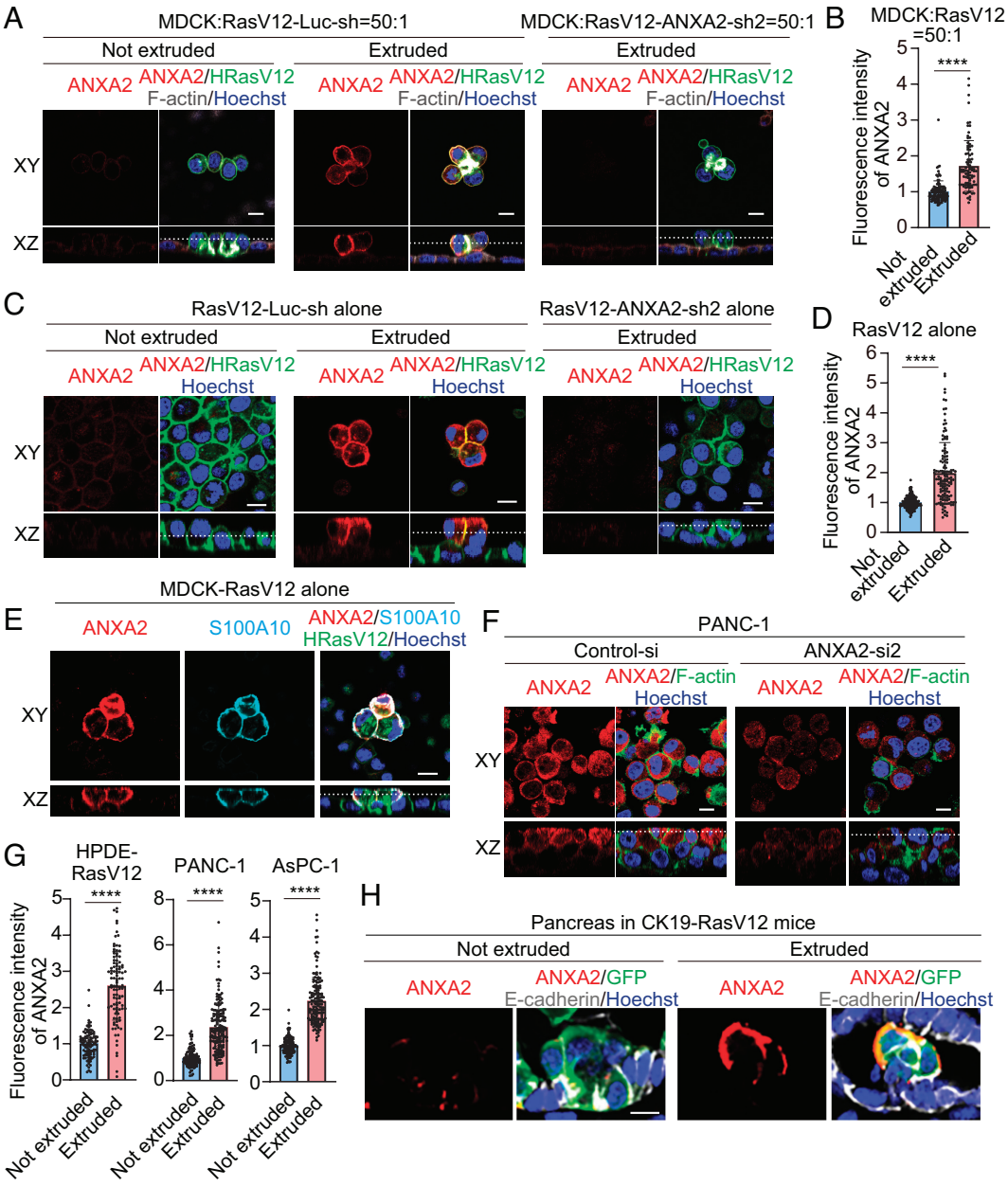

Fig. 2. ANXA2 is accumulated in apically extruded, transformed cells. (*A*) Immunofluorescence images of ANXA2 in apically extruded RasV12 cells. MDCK-pTR GFP-RasV12 Luc-shRNA or ANXA2-shRNA2 cells were cocultured with normal MDCK cells. After 24 h of doxycycline treatment, cells were stained with anti-ANXA2 antibody (red), Alexa Fluor 647-conjugated phalloidin (gray), and Hoechst (blue). (*B*) Quantification of the fluorescence intensity of ANXA2 in MDCK-pTR GFP-RasV12 Luc-shRNA cells in (*A*). Values are expressed as a ratio relative to Not extruded. Data are mean ± SD. ****$P < 0.0001$ (Mann–Whitney test); n = 103 and 86 cells from three independent experiments. (*C–F*) Immunofluorescence analyses of ANXA2. (*C*, *E*, and *F*) Immunofluorescence images of ANXA2 in apically delaminated RasV12 cells (*C* and *E*) and PANC-1 cells (*F*) under the single culture condition. MDCK-pTR GFP-RasV12 (*C* and *E*) or PANC-1 cells (*F*) were cultured alone and stained with anti-ANXA2 antibody (red), Hoechst (blue), and/or Alexa Fluor 488-conjugated phalloidin (green). (*E*) Cells were also stained with anti-S100A10 antibody (cyan) to examine the colocalization of ANXA2 and S100A10. (*D*) Quantification of the fluorescence intensity of ANXA2 in MDCK-pTR GFP-RasV12 Luc-shRNA cells in (*C*). Values are expressed as a ratio relative to Not extruded. Data are mean ± SD. ****$P < 0.0001$ (Mann–Whitney test); n = 171 and 130 cells from three independent experiments. (*G*) Quantification of the fluorescence intensity of ANXA2 in HPDE-pTRE3G GFP-KRasV12, PANC-1, and AsPC-1 cells. Values are expressed as a ratio relative to Not extruded. Data are mean ± SD. ****$P < 0.0001$ (Mann–Whitney test); n = 100 and 104 cells for HPDEC-RasV12, n = 121 and 167 cells for PANC-1, n = 133 and 152 cells for AsPC-1 from three independent experiments. Representative images of HPDE-pTRE3G GFP-KRasV12 and AsPC-1 cells are shown in *SI Appendix*, Fig. S2 *B* and *C*. (*H*) Immunofluorescence images of ANXA2 in apically extruded RasV12-expressing cells in the murine pancreatic epithelium. At 7 d after tamoxifen administration, the pancreatic tissue samples from CK19-RasV12-GFP mice were stained with anti-ANXA2 (red), anti-GFP (green), and anti-E-cadherin (gray) antibodies, and Hoechst (blue). [Scale bars, 10 μm (*A*, *C*, *E*, *F*, and *H*).]

to a similar extent to apically extruded RasV12 cells (*SI Appendix*, Fig. S4 *A–D*), suggesting that oncogenic signals are not required for the accumulation of S100A10 or ANXA2 and that the process of apical cell extrusion per se triggers their accumulation.

Previous studies have demonstrated that S100A10 forms a heterotetrameric complex with ANXA2 and that the absence of ANXA2 posttranscriptionally destabilizes S100A10 (25). Accordingly, we showed by western blotting that knockdown of ANXA2 strongly reduced the expression of S100A10 in RasV12-transformed MDCK cells or PANC-1 cells (Fig. 3 *A* and *C*). In contrast, knockdown of S100A10 did not affect the expression level of ANXA2 (Fig. 3 *B* and *D*). In addition, immunofluorescence analyses demonstrated that knockdown of ANXA2 profoundly diminished S100A10 immunofluorescence in apically extruded MDCK-RasV12 cells or

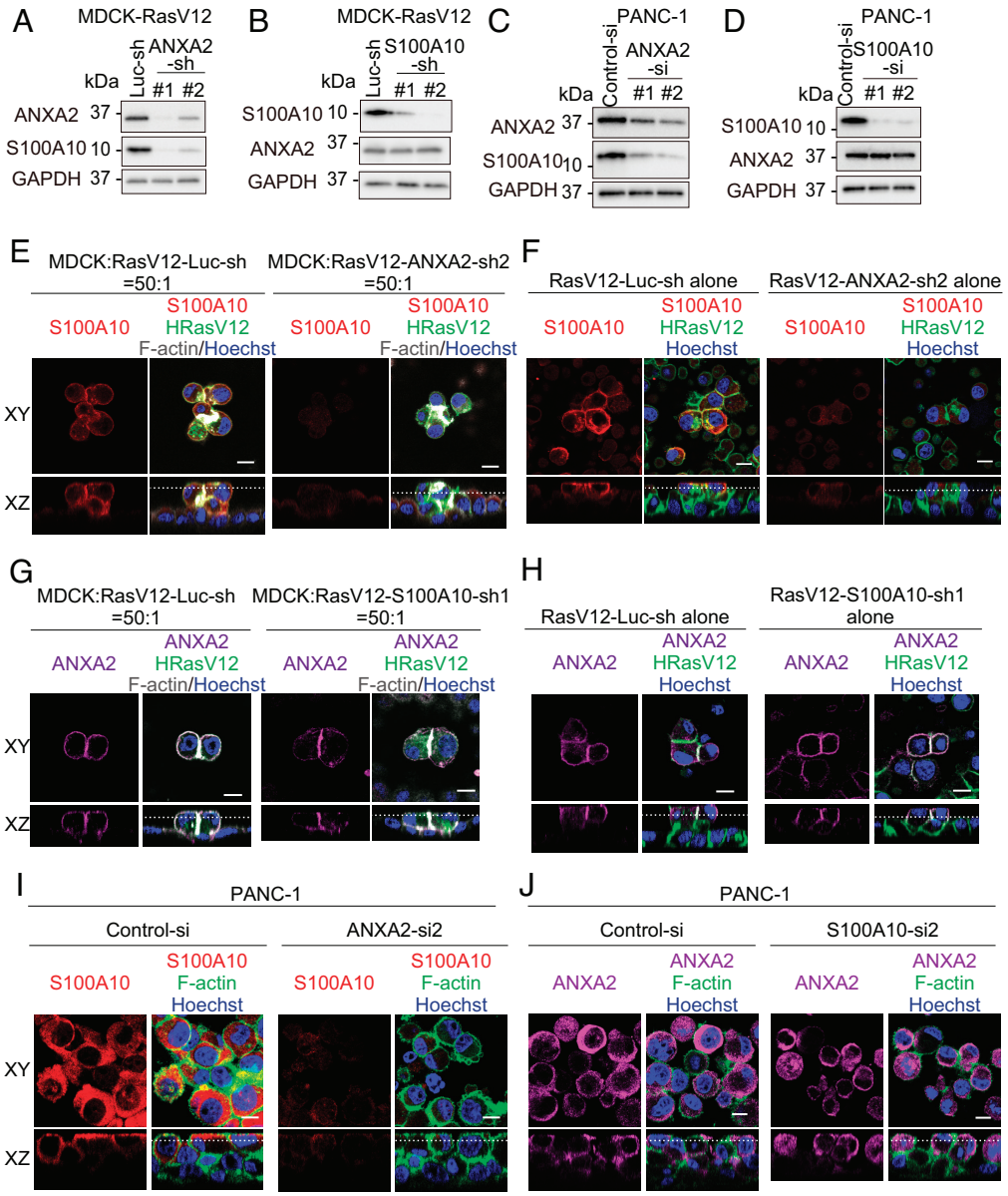

Fig. 3. ANXA2 acts upstream of S100A10. (*A–D*) Immunoblotting analyses for the effect of knockdown of ANXA2 (*A* and *C*) or S100A10 (*B* and *D*) on the expression of ANXA2 and S100A10. MDCK-pTR GFP-RasV12 Luc-shRNA, ANXA2-shRNA1 or 2 (*A*), or S100A10-shRNA1 or 2 (*B*) cells, or PANC-1 cells transfected with control-siRNA, ANXA2-siRNA1 or 2 (*C*), or S100A10-siRNA1 or 2 (*D*) were cultured alone. Cell lysates were analyzed by western blotting with anti-ANXA2, anti-S100A10, or anti-GAPDH antibody. (*E–J*) Immunofluorescence analyses for the effect of knockdown of ANXA2 or S100A10 on the accumulation of S100A10 or ANXA2 in apically extruded transformed cells. (*E–H*) MDCK-pTR GFP-RasV12 Luc-shRNA, ANXA2-shRNA2 (*E* and *F*), or S100A10-shRNA1 (*G* and *H*) cells were cocultured with normal MDCK cells (*E* and *G*) or cultured alone (*F* and *H*). (*I* and *J*) PANC-1 cells transfected with control-siRNA, ANXA2-siRNA2 (*I*), or S100A10-siRNA2 (*J*) were cultured alone. (*E–J*) Cells were stained with anti-S100A10 antibody (red), anti-ANXA2 antibody (magenta), Hoechst (blue), and/or Alexa Fluor 647- or 488-conjugated phalloidin (gray or green). [Scale bars, 10 μm (*E–J*).]

PANC-1 cells, whereas knockdown of S100A10 did not substantially influence ANXA2 staining (Fig. 3 *E–J*). Collectively, these results indicate that ANXA2 is required for and thus acts upstream of S100A10 accumulation and that the accumulation of S100A10 is regulated at both transcriptional and post-translational levels.

Knockdown of ANXA2 Promotes Apoptosis of Apically Extruded RasV12-Transformed Cells. While analyzing the effect of ANXA2 knockdown in MDCK cells, we realized that ANXA2-knockdown RasV12 cells often died after apical extrusion. To examine the occurrence of apoptosis, we used NucView, a fluorescence apoptosis sensor, to monitor caspase activity in live images (36). We found that knockdown of ANXA2 in RasV12 cells significantly increased the NucView-positive ratio in apically extruded RasV12 cells under the coculture condition with normal cells (Fig. 4 *A* and *B*). In addition, the NucView-positive ratio was profoundly elevated in apically delaminated ANXA2-knockdown RasV12 cells under the single culture condition (Fig. 4 *C* and *D*). Accordingly, knockdown of ANXA2 in RasV12 cells substantially diminished the area of the bilayered epithelium bearing apically delaminated cells (Fig. 4 *E* and *F*). Similarly, knockdown of S100A10 also suppressed the formation of the bilayered regions (Fig. 4 *E* and *F*). When normal MDCK cells were cultured alone at high cell density, all analyzed apically extruded normal cells were NucView-positive (n = 20) (*SI Appendix*, Fig. S5*A*), and the bilayered regions were not observed (Fig. 4*F*). Together with *SI Appendix*, Fig. S4 *A–D*, these results suggest that the accumulation of ANXA2 and S100A10 is not sufficient to prevent apically extruded cells from undergoing apoptosis; instead, oncogenic

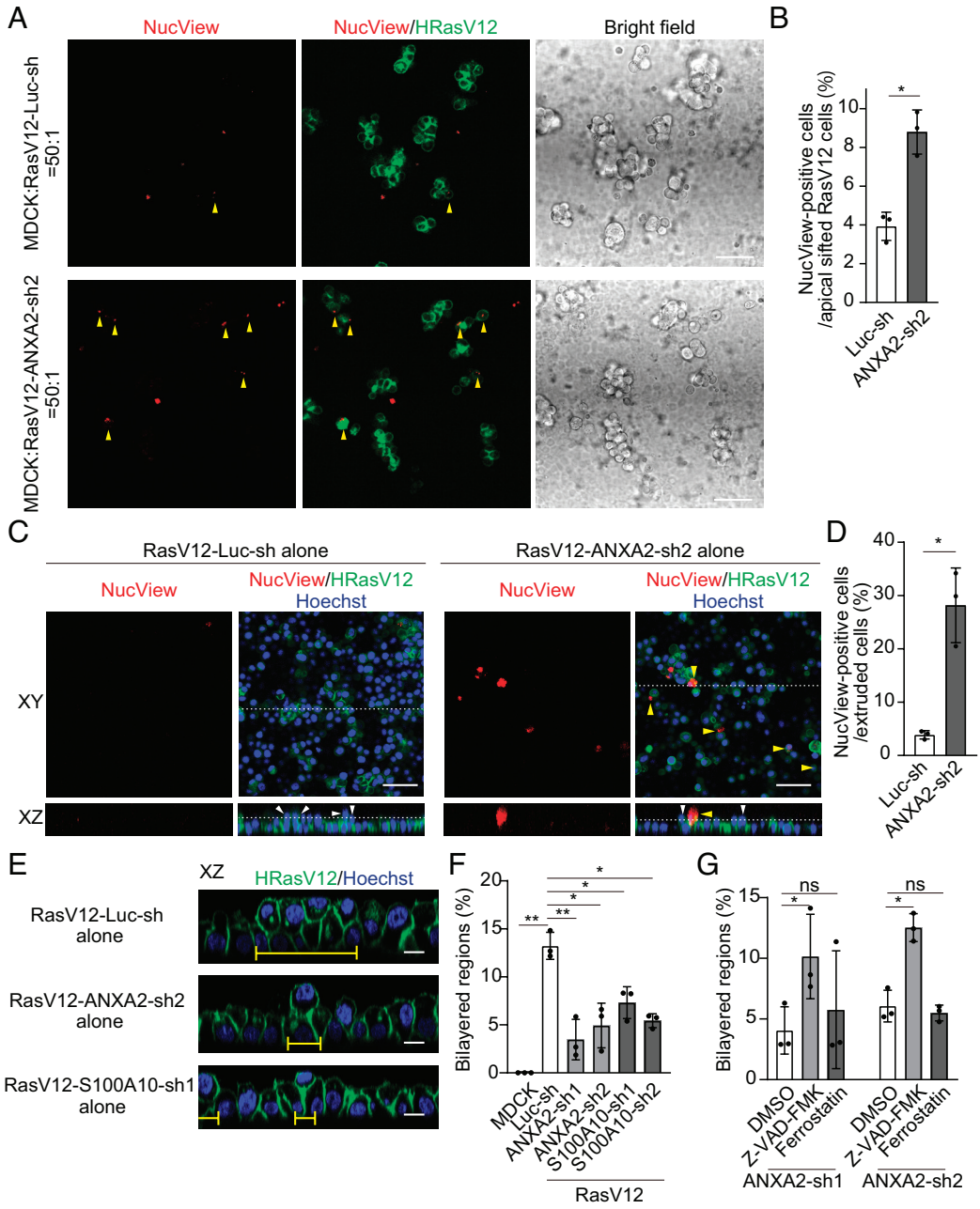

Fig. 4. Knockdown of ANXA2 promotes apoptosis of apically extruded RasV12-transformed cells. (*A–D*) NucView analyses for apically extruded RasV12 cells. MDCK-pTR GFP-RasV12 Luc-shRNA or ANXA2-shRNA2 cells were cocultured with normal MDCK cells (*A*) or cultured alone (*C*) and stained with NucView 530 (red). Yellow and white arrowheads indicate NucView-positive and -negative, extruded RasV12 cells, respectively. (*B* and *D*) Quantification of the ratio of NucView-positive cells in apically shifted/extruded RasV12 cells in (*A*) and (*C*). (*B*) Note that the number of NucView-positive surrounding normal cells is very few. Only NucView-positive GFP-RasV12-expressing cells were analyzed. Data are mean ± SD from three independent experiments. **P* < 0.05 (paired two-tailed Student's test). The total number of analyzed extruded cells is 1,043 and 766 (*B*) or 491 and 257 (*D*) from three independent experiments. (*E*) XZ-images of MDCK-pTR GFP-RasV12 Luc-shRNA, ANXA2-shRNA2, or S100A10-shRNA1 cells. Yellow lines indicate the bilayered regions. (*F*) Effect of knockdown of ANXA2 or S100A10 on the formation of bilayered epithelia. Normal MDCK, MDCK-pTR GFP-RasV12 Luc-shRNA, ANXA2-shRNA1 or 2, or S100A10-shRNA1 or 2 cells were cultured alone, and the bilayered regions were quantified from XZ-images. Data are mean ± SD from three independent experiments. **P* < 0.05 and ***P* < 0.01 (one-way ANOVA with Dunnett's test). (*G*) Effect of cell death inhibitors on the formation of bilayered epithelia of ANXA2-knockdown RasV12 cells. MDCK-pTR GFP-RasV12 ANXA2-shRNA1 or 2 cells were cultured alone and treated with Z-VAD-FMK or Ferrostatin-1. Data are mean ± SD. **P* < 0.05; ns, not significant (one-way ANOVA with Dunnett's test). [Scale bars, 50 μm (*A* and *C*) and 10 μm (*E*).]

signals are also required. Knockdown of either ANXA2 or S100A10 did not suppress proliferation of RasV12 cells (*SI Appendix*, Fig. S5 *B* and *C*), implying that the effect of knockdown on bilayered structures is not due to decreased cell proliferation. When ANXA2-knockdown RasV12 cells were treated with apoptosis inhibitor Z-VAD-FMK, the formation of bilayered epithelial structures was restored (Fig. 4*G*). In contrast, the treatment with ferroptosis inhibitor Ferrostatin had no effect (Fig. 4*G*). These results suggest that the accumulated ANXA2 suppresses apoptosis of apically extruded RasV12-transformed cells.

Apically Extruded ANXA2-Knockdown RasV12-Transformed Cells Undergo ROS-Mediated Apoptosis through p38MAPK Activation. Previous studies have demonstrated that the level of intracellular ROS increases in apically extruded cells from the epithelial monolayer (10). The increased ROS induce anoikis in apically extruded normal cells (37). In contrast, transformed cells are resistant to the ROS-mediated stress and able to survive upon apical extrusion (10). We then examined the ROS level using CellROX Orange, a cumulative fluorescence probe of intracellular

ROS. The fluorescence intensity of CellROX was substantially elevated in apically extruded RasV12 cells compared with nonextruded RasV12 cells (Fig. 5 *A* and *B*). The CellROX intensity was further moderately increased in ANXA2-knockdown RasV12 cells (Fig. 5 *A* and *B*), suggesting that ANXA2 suppresses the ROS level in apically extruded RasV12 cells. Next, we examined the effect of the ROS scavenger Trolox. First, we confirmed that the Trolox treatment diminished CellROX fluorescence in apically extruded RasV12 cells (Fig. 5*C*). Trolox significantly reduced the NucView-positive ratio in apically extruded ANXA2-knockdown

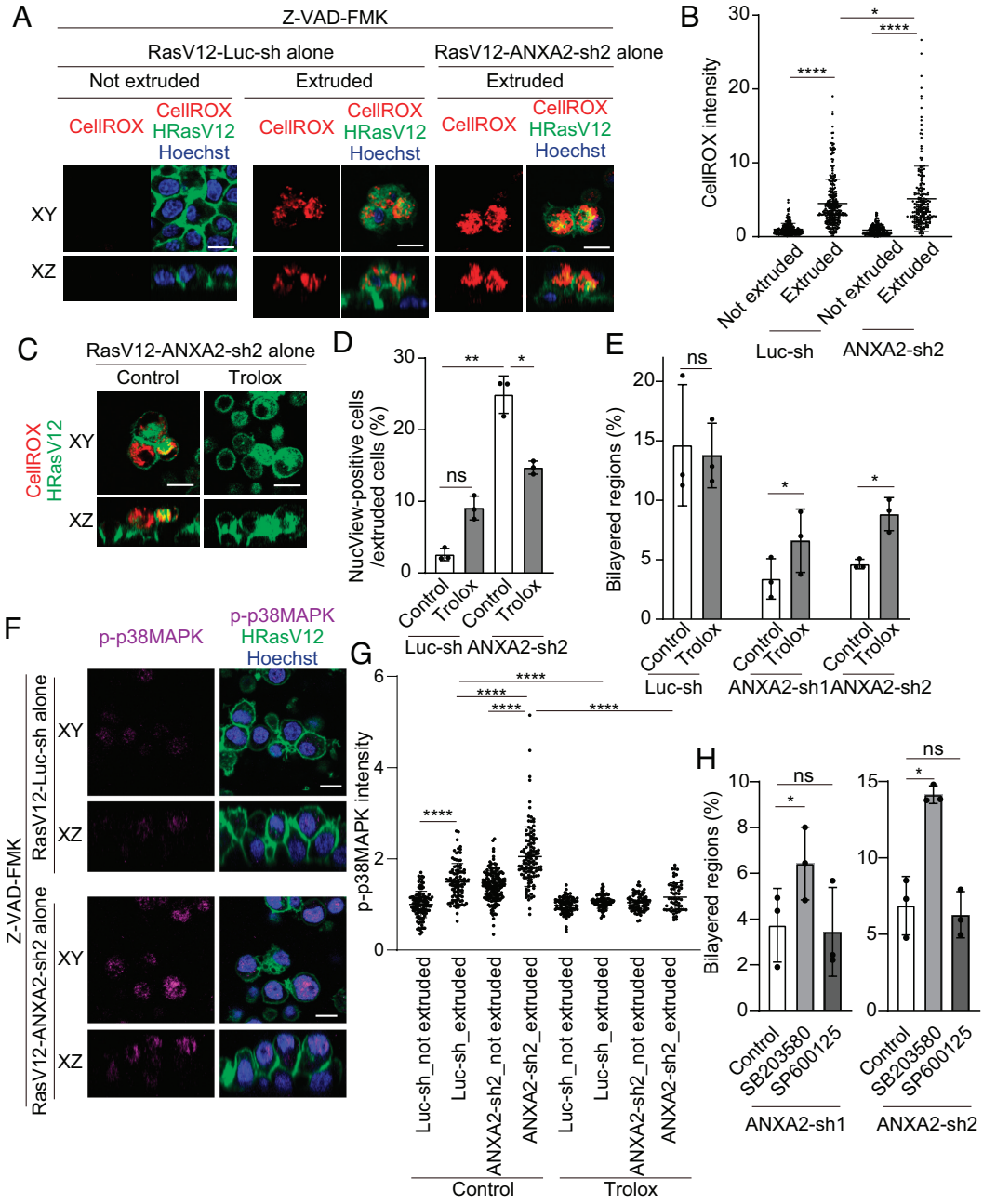

Fig. 5. The ROS-p38MAPK pathway positively regulates apoptosis in extruded ANXA2-knockdown RasV12-transformed cells. (*A*) Fluorescence images of CellROX in apically extruded RasV12 cells. MDCK-pTR GFP-RasV12 Luc-shRNA or ANXA2-shRNA2 cells were cultured alone in the presence of Z-VAD-FMK and stained with CellROX (red) and Hoechst (blue). (*B*) Quantification of the fluorescence intensity of CellROX in (*A*). Values are expressed as a ratio relative to Not extruded Luc-sh. Data are mean ± SD. **P* < 0.05, *****P* < 0.0001 (one-way ANOVA with Dunnett's test); n = 227, 282, 176, and 203 cells from four independent experiments. (*C*) The effect of Trolox on CellROX fluorescence in apically extruded ANXA2-knockdown RasV12 cells. (*D*) Quantification of the ratio of NucView-positive cells in apically extruded RasV12 cells. MDCK-pTR GFP-RasV12 Luc-shRNA or ANXA2-shRNA2 cells were cultured with or without Trolox and analyzed with NucView. Data are mean ± SD from three independent experiments. **P* < 0.05, ***P* < 0.01; ns, not significant (one-way ANOVA with Dunnett's test). The total number of analyzed extruded cells is 322, 374, 215, and 341 from three independent experiments. (*E*) Effect of Trolox on the formation of bilayered epithelia of ANXA2-knockdown RasV12 cells. MDCK-pTR GFP-RasV12 Luc-shRNA, ANXA2-shRNA1 or 2 cells were cultured with Trolox. Data are mean ± SD from three independent experiments. **P* < 0.05; ns, not significant. Paired two-tailed Student's test. (*F*) Immunofluorescence images of phosphorylated p38MAPK (p-p38MAPK) in apically extruded RasV12 cells. (*G*) Quantification of p-p38MAPK immunofluorescence intensity. (*F* and *G*) MDCK-pTR GFP-RasV12 Luc-shRNA or ANXA2-shRNA2 cells were cultured with or without Trolox in the presence of Z-VAD-FMK and stained with anti-p-p38MAPK antibody (magenta) and Hoechst (blue). (*G*) Values are expressed as a ratio relative to control Luc-sh_Not extruded. Data are mean ± SD. *****P* < 0.0001 (one-way ANOVA with Dunnett's test); n = 110, 99, 159, 114, 91, 81, 74, and 56 cells from three independent experiments. (*H*) Effect of p38MAPK inhibitor or JNK inhibitor on the formation of bilayered epithelia of ANXA2-knockdown RasV12 cells. MDCK-pTR GFP-RasV12 ANXA2-shRNA1 or 2 cells were cultured with p38MAPK inhibitor (SB203580) or JNK inhibitor (SP600125). Data are mean ± SD from three independent experiments. **P* < 0.05; ns, not significant. One-way ANOVA with Dunnett's test. [Scale bars, 10 μm (*A*, *C*, and *F*).]

RasV12 cells (Fig. 5*D*). Furthermore, the Trolox treatment, at least partially, restored the formation of bilayered epithelia of ANXA2-knockdown RasV12 cells (Fig. 5*E*). Trolox did not influence the accumulation of ANXA2 or S100A10 in apically delaminated RasV12 cells (*SI Appendix*, Fig. S6 *A* and *B*). These data indicate that the increased ROS contribute to the induction of apoptosis in apically extruded ANXA2-knockdown RasV12 cells.

We next explored the molecular mechanism of how increased ROS induce apoptosis in ANXA2-knockdown RasV12 cells. Previous studies reported the functional link between ANXA2 and several stress-response regulators including p38MAPK, c-Jun N-terminal kinase (JNK), and p53 (38, 39). We found that phosphorylation of p38MAPK was enhanced in apically delaminated RasV12 cells, which was further promoted in ANXA2-knockdown RasV12 cells (Fig. 5 *F* and *G*). The Trolox treatment significantly diminished the level of phosphorylation of p38MAPK in apically extruded RasV12 cells (Fig. 5*G* and *SI Appendix*, Fig. S6*C*). Moreover, p38MAPK inhibitor SB203580, but not JNK inhibitor SP600125 or p53 inhibitor Pifithrin-α, significantly promoted the formation of bilayered epithelia of ANXA2-knockdown RasV12 cells (Fig. 5*H* and *SI Appendix*, Fig. S6*D*). Collectively, these data suggest that accumulated ANXA2 suppresses the p38MAPK activity in apically extruded transformed cells, thereby blocking the induction of apoptosis (Fig. 6).

Discussion

In this study, we demonstrate that ANXA2 and S100A10 accumulate in apically extruded transformed cells from the epithelial monolayer, which can be observed in multiple experimental systems, including RasV12- or Src-transformed MDCK cells, RasV12-transformed HPDE cells, pancreatic cancer cells, and mouse pancreatic ductal and lung bronchial epithelia. Thus, the accumulation of ANXA2/S100A10 is a general phenomenon that occurs both in vitro and in vivo. However, it still remains obscure how ANXA2/S100A10 accumulate in the apically extruded transformed cells. Trolox treatment does not suppress the accumulation of ANXA2/S100A10, suggesting that the upregulation of ANXA2/S100A10 is not caused by the increased ROS. Previous studies have demonstrated that ANXA2/S100A10 preferentially localize at cholesterol-rich lipid rafts (40–42). Using fluorescence-conjugated lysenin that specifically bound to lipid rafts, we have found that the formation of lipid rafts is promoted in apically extruded RasV12 cells that are surrounded by normal cells (*SI Appendix*, Fig. S7*A*) or cultured alone (*SI Appendix*, Fig. S7*B*). Treatment with methyl-β-cyclodextrin (MβCD) that disrupts lipid rafts by removing cholesterol from the plasma membrane diminishes the lysenin fluorescence in the apically extruded cells (*SI Appendix*, Fig. S7*B*). The MβCD treatment induces the release of ANXA2 or S100A10 from the plasma membrane to the cytosol but does not reduce the up-regulated expression of ANXA2/S100A10 (*SI Appendix*, Fig. S7 *C–F*). These data indicate that lipid rafts regulate the membrane localization of ANXA2/S100A10 in apically extruded cells, but their accumulation is mediated by other upstream regulators. The accumulation of ANXA2/S100A10 is observed in apically extruded cells but not in apically extruding cells. In addition, the mRNA expression level of ANXA2/S100A10 is comparable under the adherent and nonadherent conditions. Hence, the detachment from the basal substratum is required but not sufficient for the upregulation of ANXA2/S100A10. Furthermore, the ANXA2/S100A10 accumulation occurs not only in apically extruded transformed cells but also in apically extruded normal cells, suggesting that not the oncogenic signals but the process of apical extrusion per se triggers the accumulation of ANXA2/S100A10. Apical cell extrusion is a complex phenomenon that comprises multiple processes including the detachment from the basal substratum, a loss of intercellular adhesions with neighboring cells, the attachment to the apical surface of the underlying cells, and exposure to the physical insults within the apical luminal space. The upstream regulators for ANXA2/S100A10 still remain to be identified.

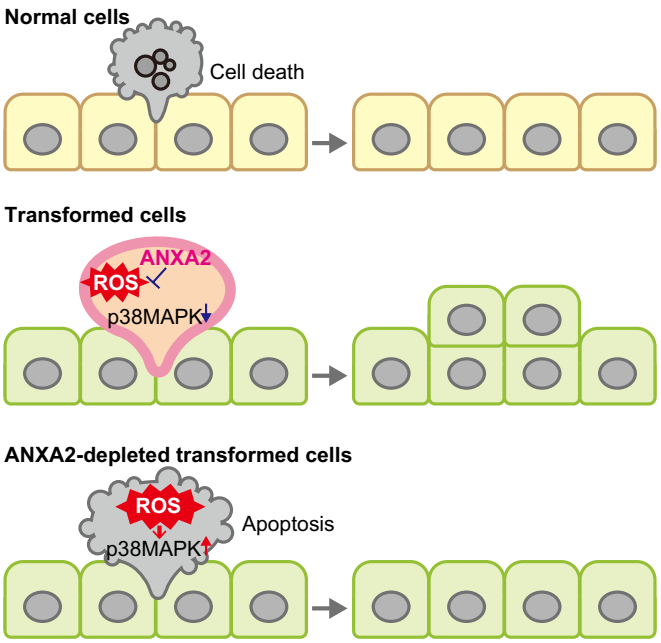

Fig. 6. Schematics for the functional role of ANXA2 in apically extruded transformed cells. Accumulated ANXA2 suppresses the ROS-mediated activation of p38MAPK and induction of apoptosis, leading to the formation of multilayered epithelia.

The results shown in this study indicate that accumulated ANXA2/S100A10 suppress ROS-mediate apoptosis in extruded transformed cells. Knockdown of ANXA2 moderately increased the ROS level in apically extruded transformed cells, which is compatible with previous studies that ANXA2 can quench ROS (43). Additionally, knockdown of ANXA2 substantially increases phosphorylation of p38MAPK; it is thus plausible that ANXA2 not only affects the ROS level but also somehow suppresses the ROS-mediated activation of p38MAPK. Previous studies have demonstrated that ROS can induce p38MAPK phosphorylation through activation of apoptosis signal-regulating kinase (ASK)1 (44, 45). However, knockdown of ASK1 did not significantly suppress the phosphorylation of p38MAPK in extruded ANXA2-knockdown RasV12 cells (*SI Appendix*, Fig. S8 *A* and *B*). Although the negative result with ASK1 siRNA oligos could be caused by incomplete knockdown of ASK1, it is possible that other upstream kinases are involved in the ROS-mediated activation of p38MAPK, potentially working in combination. It needs to be further examined how ANXA2 regulates the ROS-p38MAPK pathway in apically extruded cells.

It has been recently reported that the cell detachment from the basal substratum can induce not only apoptosis but also ferroptosis (46–48). In a previous study, we have shown that the expression of COL17A1 and CD44 is profoundly up-regulated at the upper layers of multilayered, transformed epithelia (18). Depletion of COL17A1 or CD44 suppresses the occurrence of ferroptosis of the apically delaminated transformed cells, suggesting that the accumulated COL17A1 and CD44 suppress ferroptosis at the upper layer of the multilayered epithelial structures. As shown in *SI Appendix*, Fig. S9 *A* and *B*, knockdown of CD44 does not affect the accumulation of ANXA2/S100A10, and vice versa. Taken together, those results

imply that upon apical extrusion, cancerous cells could be endowed with both antiapoptotic and antiferroptotic machineries, facilitating the formation of multilayered epithelia.

Expression of ANXA2 and S100A10 is often up-regulated in various types of cancer including pancreatic, colorectal, breast, and ovarian cancer (28, 29). The higher expression level of ANXA2/S100A10 is correlated to poor prognosis (49–51). The increased expression of ANXA2/S100A10 confers antiapoptotic properties on malignant tumor cells, potentially leading to resistance against chemotherapy or radiotherapy (30, 38, 39, 52, 53). Here, we demonstrate that ANXA2/S100A10 positively regulate the formation of multilayered and transformed epithelia that are often observed at the earlier stage of carcinogenesis. Hence, ANXA2/S100A10 can be potential therapeutic targets to prevent the development of precancerous lesions. In future studies, the molecular mechanisms of ANXA2/S100A10 accumulation in apically delaminated transformed cells need to be further explored, which would lead to the establishment of novel cancer preventive treatments.

Materials and Methods

Materials, cell culture and RNA interference, phage antibody display screening, immunofluorescence and western blotting, immunoprecipitation and mass spectrometry, quantitative real-time PCR, in situ hybridization assay, CellROX assay, NucView imaging, mice, and quantification and statistical analysis are described in *SI Appendix, Materials and Methods*.

Data, Materials, and Software Availability. All study data are included in the article and/or *SI Appendix*. All study data are deposited in the following repository https://moloncresearcherinfo.net/Statistical source data.xlsx and available upon request.

ACKNOWLEDGMENTS. We acknowledge support from Japan Society for the Promotion of Science (JSPS) Grant-in-Aid for Scientific Research on Transformative Research Areas (A) 21H05285A01, Grant-in-Aid for Scientific Research (S) 21H05039, JSPS Bilateral Joint Research Projects (The Royal Society) JPJSBP1 20215703, Japan Science and Technology Agency (Moonshot Research & Development: Grant Number JPMJPS2022), the Takeda Science Foundation, and SAN-ESU GIKEN CO. LTD (to Y.F.), and JSPS Grant-in-Aid for Scientific Research (C) 20K07630 (to S. Ito).

Author affiliations: [a]Department of Molecular Oncology, Kyoto University Graduate School of Medicine, Kyoto 606-8501, Japan; [b]Eisai Co., Ltd., Kobe 650-0047, Japan; [c]Protein Targeting Biologics, KAN Research Institute, Kobe 650-0047, Japan; [d]Division of Molecular Oncology, Institute for Genetic Medicine, Hokkaido University Graduate School of Chemical Sciences and Engineering, Sapporo 060-0815, Japan; [e]Department of Biology, Faculty of Sciences, Kyushu University, Fukuoka 819-0395, Japan; and [f]Laboratory of Cell Signaling, Graduate School of Pharmaceutical Sciences, The University of Tokyo, Tokyo 113-0033, Japan

1. A. M. Marchiando, W. V. Graham, J. R. Turner, Epithelial barriers in homeostasis and disease. *Annu. Rev. Pathol.* **5**, 119–144 (2010).
2. L. W. Peterson, D. Artis, Intestinal epithelial cells: Regulators of barrier function and immune homeostasis. *Nat. Rev. Immunol.* **14**, 141–153 (2014).
3. C. E. Buckley, D. St Johnston, Apical-basal polarity and the control of epithelial form and function. *Nat. Rev. Mol. Cell Biol.* **23**, 559–577 (2022).
4. G. T. Eisenhoffer *et al.*, Crowding induces live cell extrusion to maintain homeostatic cell numbers in epithelia. *Nature* **484**, 546–549 (2012).
5. E. Marinari *et al.*, Live-cell delamination counterbalances epithelial growth to limit tissue overcrowding. *Nature* **484**, 542–545 (2012).
6. C. Hogan *et al.*, Characterization of the interface between normal and transformed epithelial cells. *Nat. Cell Biol.* **11**, 460–467 (2009).
7. S. Kon *et al.*, Cell competition with normal epithelial cells promotes apical extrusion of transformed cells through metabolic changes. *Nat. Cell Biol.* **19**, 530–541 (2017).
8. F. G. Giancotti, E. Ruoslahti, Integrin signaling. *Science* **285**, 1028–1032 (1999).
9. D. G. Stupack, D. A. Cheresh, Get a ligand, get a life: Integrins, signaling and cell survival. *J. Cell Sci.* **115**, 3729–3738 (2002).
10. Z. T. Schafer *et al.*, Antioxidant and oncogene rescue of metabolic defects caused by loss of matrix attachment. *Nature* **461**, 109–113 (2009).
11. L. Galluzzi *et al.*, Molecular mechanisms of cell death: Recommendations of the nomenclature committee on cell death 2018. *Cell Death Differ.* **25**, 486–541 (2018).
12. C. L. Buchheit, K. J. Weigel, Z. T. Schafer, Cancer cell survival during detachment from the ECM: Multiple barriers to tumour progression. *Nat. Rev. Cancer* **14**, 632–641 (2014).
13. S. M. Frisch, H. Francis, Disruption of epithelial cell-matrix interactions induces apoptosis. *J. Cell Biol.* **124**, 619–626 (1994).
14. S. M. Frisch, R. A. Screaton, Anoikis mechanisms. *Curr. Opin. Cell Biol.* **13**, 555–562 (2001).
15. J. A. Mason *et al.*, Oncogenic Ras differentially regulates metabolism and anoikis in extracellular matrix-detached cells. *Cell Death Differ.* **23**, 1271–1282 (2016).
16. A. McFall *et al.*, Oncogenic Ras blocks anoikis by activation of a novel effector pathway independent of phosphatidylinositol 3-kinase. *Mol. Cell Biol.* **21**, 5488–5499 (2001).
17. Y. Moller *et al.*, Oncogenic Ras triggers hyperproliferation and impairs polarized colonic morphogenesis by autocrine ErbB3 signaling. *Oncotarget* **7**, 53526–53539 (2016).
18. K. Kozawa *et al.*, The CD44/COL17A1 pathway promotes the formation of multilayered, transformed epithelia. *Curr. Biol.* **31**, 3086–3097.e7 (2021).
19. A. Nyga *et al.*, Oncogenic RAS instructs morphological transformation of human epithelia via differential tissue mechanics. *Sci. Adv.* **7**, eabg6467 (2021).
20. X. Q. Wang *et al.*, Oncogenic K-Ras regulates proliferation and cell junctions in lung epithelial cells through induction of cyclooxygenase-2 and activation of metalloproteinase-9. *Mol. Biol. Cell* **20**, 791–800 (2009).
21. V. Gerke, C. E. Creutz, S. E. Moss, Annexins: Linking Ca2+ signalling to membrane dynamics. *Nat. Rev. Mol. Cell Biol.* **6**, 449–461 (2005).
22. V. Gerke, S. E. Moss, Annexins: From structure to function. *Physiol. Rev.* **82**, 331–371 (2002).
23. S. Rety *et al.*, The crystal structure of a complex of p11 with the annexin II N-terminal peptide. *Nat. Struct. Biol.* **6**, 89–95 (1999).
24. D. M. Waisman, Annexin II tetramer: Structure and function. *Mol. Cell Biochem.* **149-150**, 301–322 (1995).
25. A. Puisieux, J. Ji, M. Ozturk, Annexin II up-regulates cellular levels of p11 protein by a post-translational mechanisms. *Biochem. J.* **313**, 51–55 (1996).
26. J. S. Seo, P. Svenningsson, Modulation of ion channels and receptors by p11 (S100A10). *Trends Pharmacol. Sci.* **41**, 487–497 (2020).
27. U. Rescher, V. Gerke, S100A10/p11: Family, friends and functions. *Pflugers Arch.* **455**, 575–582 (2008).
28. T. M. Noye, N. A. Lokman, M. K. Oehler, C. Ricciardelli, S100A10 and cancer hallmarks: Structure, functions, and its emerging role in ovarian cancer. *Int. J. Mol. Sci.* **19**, 4122 (2018).
29. M. V. Christensen, C. K. Hogdall, K. M. Jochumsen, E. V. S. Hogdall, Annexin A2 and cancer: A systematic review. *Int. J. Oncol.* **52**, 5–18 (2018).
30. H. Jung *et al.*, Intracellular annexin A2 regulates NF-kappaB signaling by binding to the p50 subunit: Implications for gemcitabine resistance in pancreatic cancer. *Cell Death Dis.* **6**, e1606 (2015).
31. S. Y. Hsu, A. Kaipia, L. Zhu, A. J. Hsueh, Interference of BAD (Bcl-xL/Bcl-2-associated death promoter)-induced apoptosis in mammalian cells by 14-3-3 isoforms and P11. *Mol. Endocrinol.* **11**, 1858–1867 (1997).
32. Y. Huang *et al.*, Involvement of annexin A2 in p53 induced apoptosis in lung cancer. *Mol. Cell Biochem.* **309**, 117–123 (2008).
33. S. Suzuki, Y. Yamayoshi, A. Nishimuta, Y. Tanigawara, S100A10 protein expression is associated with oxaliplatin sensitivity in human colorectal cancer cells. *Proteome Sci.* **9**, 76 (2011).
34. Y. Guo, R. Li, X. Dang, S100A10 regulates tumor necrosis factor alpha-induced apoptosis in chondrocytes via the reactive oxygen species/nuclear factor-kappa B pathway. *Biotechnol. Appl. Biochem.* **69**, 2284–2295 (2022).
35. A. Sasaki *et al.*, Obesity suppresses cell-competition-mediated apical elimination of RasV12-transformed cells from epithelial tissues. *Cell Rep.* **23**, 974–982 (2018).
36. H. Cen, F. Mao, I. Aronchik, R. J. Fuentes, G. L. Firestone, DEVD-NucView488: A novel class of enzyme substrates for real-time detection of caspase-3 activity in live cells. *FASEB J.* **22**, 2243–2252 (2008).
37. A. E. Li *et al.*, A role for reactive oxygen species in endothelial cell anoikis. *Circ. Res.* **85**, 304–310 (1999).
38. H. He *et al.*, Knockdown of annexin A2 enhances radiosensitivity by increasing G2/M-phase arrest, apoptosis and activating the p38 MAPK-HSP27 pathway in nasopharyngeal carcinoma. *Front. Oncol.* **12**, 769544 (2022).
39. X. Feng *et al.*, Annexin A2 contributes to cisplatin resistance by activation of JNK–p53 pathway in non-small cell lung cancer cells. *J. Exp. Clin. Cancer Res.* **36**, 123 (2017).
40. T. Harder, R. Kellner, R. G. Parton, J. Gruenberg, Specific release of membrane-bound annexin II and cortical cytoskeletal elements by sequestration of membrane cholesterol. *Mol. Biol. Cell* **8**, 533–545 (1997).
41. S. Oliferenko *et al.*, Analysis of CD44-containing lipid rafts: Recruitment of annexin II and stabilization by the actin cytoskeleton. *J. Cell Biol.* **146**, 843–854 (1999).
42. C. Benaud *et al.*, AHNAK interaction with the annexin 2/S100A10 complex regulates cell membrane cytoarchitecture. *J. Cell Biol.* **164**, 133–144 (2004).
43. P. A. Madureira *et al.*, Annexin A2 is a novel cellular redox regulatory protein involved in tumorigenesis. *Oncotarget* **2**, 1075–1093 (2011).
44. M. Saitoh *et al.*, Mammalian thioredoxin is a direct inhibitor of apoptosis signal-regulating kinase (ASK) 1. *EMBO J.* **17**, 2596–2606 (1998).
45. K. Takeda, I. Naguro, H. Nishitoh, A. Matsuzawa, H. Ichijo, Apoptosis signaling kinases: From stress response to health outcomes. *Antioxid. Redox Signal.* **15**, 719–761 (2011).
46. B. Liu *et al.*, CEMIP promotes extracellular matrix-detached prostate cancer cell survival by inhibiting ferroptosis. *Cancer Sci.* **113**, 2056–2070 (2022).
47. G. X. Wang *et al.*, DeltaNp63 inhibits oxidative stress-induced cell death, including ferroptosis, and cooperates with the BCL-2 family to promote clonogenic survival. *Cell Rep.* **21**, 2926–2939 (2017).
48. C. W. Brown, J. J. Amante, H. L. Goel, A. M. Mercurio, The α6β4 integrin promotes resistance to ferroptosis. *J. Cell Biol.* **216**, 4287–4297 (2017).
49. N. A. Lokman, C. E. Pyragius, A. Ruszkiewicz, M. K. Oehler, C. Ricciardelli, Annexin A2 and S100A10 are independent predictors of serous ovarian cancer outcome. *Transl. Res.* **171**, 83–95.e1-2 (2016).
50. M. Bydoun *et al.*, S100A10, a novel biomarker in pancreatic ductal adenocarcinoma. *Mol. Oncol.* **12**, 1895–1916 (2018).
51. X. Liu *et al.*, Overexpression of ANXA2 predicts adverse outcomes of patients with malignant tumors: A systematic review and meta-analysis. *Med. Oncol.* **32**, 392 (2015).
52. P. A. Madureira, R. Hill, P. W. Lee, D. M. Waisman, Genotoxic agents promote the nuclear accumulation of annexin A2: Role of annexin A2 in mitigating DNA damage. *PLoS One* **7**, e50591 (2012).
53. C. Y. Chen *et al.*, Targeting annexin A2 reduces tumorigenesis and therapeutic resistance of nasopharyngeal carcinoma. *Oncotarget* **6**, 26946–26959 (2015).